

# Neurostatistical imaging for diagnosing dementia: translational approach from laboratory neuroscience to clinical routine

Etsuko Imabayashi<sup>1</sup>, Tomio Inoue<sup>2</sup>

<sup>1</sup>*Integrative Brain Imaging Center, National Center of Neurology and Psychiatry, Tokyo 187-8551, Japan*

<sup>2</sup>*Department of Radiology, Yokohama City University Graduate School of Medicine and School of Medicine, Yokohama 236-0004, Japan*

Corresponding author: Etsuko Imabayashi. E-mail: [embysh@ncnp.go.jp](mailto:embysh@ncnp.go.jp)

© Shanghai Institutes for Biological Sciences, CAS and Springer-Verlag Berlin Heidelberg 2014

Statistical analysis in neuroimaging (referred to as “neurostatistical imaging”) is important in clinical neurology. Here, neurostatistical imaging and its superiority for diagnosing dementia are reviewed. In neurodegenerative dementia, the proportional distribution of brain perfusion, metabolism, or atrophy is important for understanding the symptoms and status of patients and for identifying regions of pathological damage. Although absolute quantitative changes are important in vascular disease, they are less important than relative values in neurodegenerative dementia. Even under resting conditions in healthy individuals, the distribution of brain perfusion and metabolism is asymmetrical and differs among areas. To detect small changes, statistical analysis such as the Z-score – the number of standard deviations by which a patient’s voxel value differs from the normal mean value – comparing normal controls is useful and also facilitates clinical assessment. Our recent finding of a longitudinal one-year reduction of glucose metabolism around the olfactory tract in Alzheimer’s disease using the recently-developed DARTEL normalization procedure is also presented. Furthermore, a newly-developed procedure to assess brain atrophy with CT-based voxel-based morphometry is illustrated. The promising possibilities of CT in neurostatistical imaging are also presented.

**Keywords:** neurostatistical imaging; Neurostat; 3DSSP; eZIS; VSRAD; neurodegenerative disease; CT segmentation

## Introduction

Statistical analysis in neuroimaging (described here as “neurostatistical imaging”) is crucial in clinical neurology as, for example, 3DSSP (three-dimensional stereotactic surface projections) in Neurostat<sup>[1]</sup>. Neurostatistical imaging can be applied not only to the functional imaging like brain perfusion single photon emission computed tomography (SPECT) or glucose metabolism positron emission tomography (PET), but also to morphological images like magnetic resonance imaging (MRI) with voxel-based morphometry (VBM). Useful information can be extracted by the superimposition of statistical results onto high-resolution images like MRI. Accordingly, even though

the original image resolution is low, additional anatomical information can be obtained.

## **Neuroimaging in Diagnosing Dementia**

An essential part of neuroimaging for the clinical investigation of dementia is to differentiate the underlying disease after systemic diseases have been excluded by blood chemistry or other clinical examinations. In vascular disorders of the brain, absolute quantitative regional changes are clinically important. In the same way, in brain tumors, focal information about the tissue surrounding tumors is important. In both diseases, direct inspection of the original images is useful and important. When the symptoms indicate the possibility of idiopathic normal-pressure hydrocephalus (iNPH),

not only the disproportionately enlarged subarachnoid space hydrocephalus pattern in the original morphological images, but also the distribution pattern of neurostatistical imaging are helpful for diagnosis<sup>[2]</sup>. In iNPH, neurostatistical imaging demonstrates inhomogeneity of the distribution of cerebrospinal fluid (CSF) space, which modifies the statistical results in both volumetric and functional images, according to the partial volume effect. Adjacent gray matter volume, perfusion, or metabolism is proportionally reduced if neighboring gyri are far, due to focal CSF abundance. On the contrary, these parameters are proportionally increased if neighboring gyri are closer, resulting from apparent focal CSF reduction. That is, fake significant reductions of gray matter volume, perfusion, and metabolism are observed surrounding the Sylvian fissure and ventricles and fake significant increases are observed in the area of the convexity.

### **Contribution of Neurostatistical Imaging to Neurodegenerative Dementia**

When neurodegenerative dementia is suspected, the proportional distribution of whole-brain perfusion, metabolism, or atrophy should be examined using neurostatistical imaging, because slight changes resulting from early degeneration or remote effects of that degeneration can be extracted. Even in resting conditions, the distribution of brain perfusion or metabolism in normal controls is asymmetrical and inhomogeneous. This inhomogeneity makes it difficult to assess the slight changes by visual inspection of the original tomographic images. Statistical analysis comparing normal controls makes the slight changes clear because the asymmetry and inhomogeneity in normal controls can be canceled out. In many cases of neurodegenerative disease, the changes are too obscure to detect without using neurostatistical imaging.

To diagnose the disease underlying dementia, the symptoms or status of patients are assessed, the region of pathological damage is predicted, and the dysfunction or volume loss of the lesion or remote areas is estimated. Combining the original tomographic images, neurostatistical imaging, and clinical information, the pattern of damage distribution is judged based on whether or not they match the suspected disease. Recently, more accurate analysis has been achieved due to the development of computer technology.

### **Historical Background of Neurostatistical Imaging**

In 1994, Minoshima *et al.*<sup>[3]</sup> showed that glucose metabolism decreases in the posterior cingulate in Alzheimer's disease (AD) using Neurostat (Department of Radiology, University of Washington, Seattle, WA<sup>[3]</sup>, <http://www.rad.washington.edu/research/Research/groups/nbl/neurostat-3d-ssp>). At that time, statistical parametric mapping (SPM, <http://www.fil.ion.ucl.ac.uk/spm/>) had already been developed and used for functional analysis in neuroscientific studies. Compared with SPM that had been used for statistical analysis of many subjects, the Z-score analysis in Neurostat was developed to analyze a single individual's data against a normal database obtained from many control subjects. The Z-score is calculated as: (mean voxel value of normal controls – patient voxel value) / standard deviation of normal controls. In 1997, after the launch of Donepezil (donepezil hydrochloride, E-2020, Aricept; Eisai Co., Ltd, Tokyo, Japan) as the first drug for the symptomatic treatment of AD in the UK, many imaging studies were performed to diagnose AD as early as possible. In 2001, Ohnishi *et al.*<sup>[4]</sup> applied VBM to AD patients. Subsequently, in 2004, brain amyloid deposition was visualized using PET<sup>[5]</sup>, and in 2013, even brain tau protein was observed using a PET scanner<sup>[6]</sup>.

### **Neurostatistical Imaging and Alzheimer's Disease**

#### **Findings in the Alzheimer Brain**

In neurostatistical imaging, usually images from all participants in the patient and normal control groups are anatomically standardized into the same space using templates, and voxel-based comparisons are performed to detect the specific lesions associated with the target disease. This is one of the objective methods available to avoid subjectivity and dependence on an *a priori* hypothesis, and to adopt the principle of data-driven analysis<sup>[7]</sup>.

For example, group comparison between AD patients and normal controls shows a significant decrease in glucose metabolism in the posterior cingulate and precuneus in AD<sup>[8]</sup>. Also, Kogre *et al.* reported reduced perfusion in the posterior cingulate and precuneus in very early stages of AD using <sup>99m</sup>Tc-ethylcysteinate dimer SPECT<sup>[9]</sup>.

Morphologically, because gray-matter thickness reflects the number of residual neurons, MRI has been used to derive anatomical and tissue volume information for the gray and white matter. The VBM technique maps gray-matter or white-matter loss on a voxel-by-voxel basis after anatomical standardization. In patients with AD, a significant reduction of gray-matter volume in the hippocampal formation and the entorhinal cortex has been described<sup>[4, 10]</sup>.

### **Estimation of Evidence for Diagnosis of AD Using Z-score Analysis**

As described in the former section, the Z-score is calculated as: (mean voxel value of normal controls – patient voxel value) / standard deviation of normal controls (Fig. 1). After anatomical standardization, the Z-score of each voxel in an image is calculated and superimposed on an image such as the MRI template. Before Z-score calculation, all values in voxels are globally normalized to the mean whole-brain value or the mean cerebellar value. Finally, the Z-score map of one patient compared with many normal controls is obtained, and inspection of the Z-score image is considered along with the symptoms and status.

To estimate the diagnostic accuracy of a Z-score map, a volume of interest (VOI) is placed on the Z-score map where a significant reduction was determined by

group comparison<sup>[11]</sup>. By averaging the Z-scores within the VOIs and using these values as thresholds, the receiver operating characteristic (ROC) curves discriminating patients from controls are drawn and then the accuracy is calculated. From the results, the areas that contribute most are chosen as diagnostic tools.

Evidence for the discrimination of AD from other forms of dementia has accumulated. By evaluating atrophy using three-dimensional (3D) T1 images with MRI, using the VBM method and VOIs in the hippocampus and parahippocampus, Hirata *et al.*<sup>[10]</sup> reported a discrimination accuracy of 87.8% between AD in the very early stage (amnesic type of mild cognitive impairment) and age-matched healthy controls. By evaluating the distribution of the decrease in brain glucose metabolism, Kawachi *et al.* reported an accuracy of 88.5% using VOIs in the bilateral posterior cingulate gyri and the right parietotemporal cortex<sup>[12]</sup>. Using SPECT, we reported an accuracy of 86.2% using VOIs in the posterior cingulate and precuneus<sup>[11]</sup>.

### **Evidence-based Practice for Clinical Discrimination of AD from Other Forms of Dementia**

For MRI, more than 2 000 institutes in Japan use VSRAD® (Eizai Co., Ltd.) for Z-score analysis of brain volumetry. In this software, tissue segmentation is first applied to the 3D-volume T1-weighted image, and gray-matter and white-

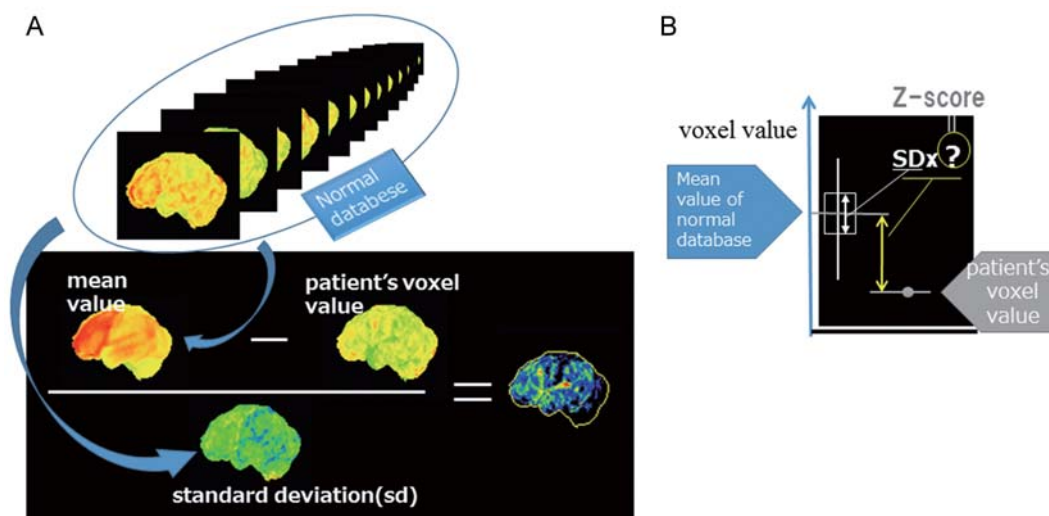


Fig. 1. Z-score analysis for diagnosis. Even with only one patient, the value can be calculated. A: Schema of Z-score calculation.  $Z\text{-score} = (\text{mean voxel value of normal controls} - \text{patient voxel value}) / \text{standard deviation of normal controls}$ . The Z-score is an absolute value that can be used both for an increase and a decrease. B: Schematic of evaluation of Z-score.

matter images are obtained from each individual. Then, diffeomorphic anatomical registration using the exponential Lie algebra (DARTE) algorithm in SPM8 is used for spatial normalization. Both gray- and white-matter atrophy can be estimated using this software.

For nuclear medicine images, in Japan, two types of software for Z-score analysis of SPECT images are mainly used, eZIS<sup>[13]</sup> (easy Z-score imaging analysis; Fujifilm RI Pharma Co., Ltd, Tokyo, Japan) and iSSP (Nihon Medi-Physics Co., Ltd, Tokyo, Japan)<sup>[14]</sup>.

eZIS includes spatial normalization parameters in SPM2. Normal databases are included in this software and inter-institutional differences can be corrected. That is, correction can be made for data obtained in the institute where the database was built, using previously-scanned phantom data. Otherwise, an original database can be built.

iSSP includes spatial normalization parameters in Neurostat. Normal databases are included and can be used as they are or an original database can be built.

The results of Z-score analysis of a suspected AD patient are shown in Fig. 2. MRI was analyzed with VSRAD®, and SPECT from the same patient was analyzed with eZIS. Voxels with significant gray-matter reduction or reduced perfusion, that is, voxels with Z-scores >2, were superimposed on the MRI template. VOIs within the areas of significant atrophy or reduced perfusion were assessed by group comparison.

### **Preparation of Normal Database**

Neuroimaging is affected by many factors, such as (1) age, race, sex, and education, (2) institution, machine, and reconstruction method, and (3) head position and functional activity during the build-up time when the functional image is obtained.

Concerning age, race, sex, and education, selection of the normal database affects the results of analysis. The more similar the conditions, the higher the sensitivity obtained. However, as the precision of subject selection increases, the size of the database decreases. As for age, if each group in the normal database consists of only a single decade, then the number is less than a database with two or three decades. In many cases, the size of the normal database is limited, and conditions are usually merged.

As for institution, machine, and reconstruction method, data acquisition should be performed in the

same way, using the same machine, with the same procedure, especially in functional imaging like SPECT and PET. When anatomical data like MRI are used for VBM, the limitation is expanded to machines with the same specifications. Concerning SPECT data, with eZIS software, inter-institutional differences can be corrected using the 3D Hoffman phantom as an intermediary. In most other cases, including other modalities like PET, an original normal database or disease control should be built. When examining the subjects, head position and brain functional activity during the build-up time should be carefully considered. In SPECT, if the tracer is injected in a bright room with the individual's eyes open, activity in the occipital region is much higher than when injected in a dark room.

Moreover, it is very important that only clinical non-image data and anatomical data are used for subject selection. The anatomical data are used for screening the space occupying lesion like infarction, tumor or hemorrhage. The functional data itself should never be used. Clinical information is of importance when choosing normal data. Normal database should not be selected only from functional image appearance, as we can hardly differentiate normal distribution from abnormal distribution with visual inspection.

## **Neurostatistical Imaging of Other Neurodegenerative Dementias**

### ***Dementia with Lewy Bodies versus AD***

Reduced occipital metabolism and perfusion or loss of dopamine transporters is used to supplement the clinical diagnosis of dementia with Lewy bodies (DLB). Recently, it has been reported that glucose metabolism in the posterior cingulate cortex in DLB<sup>[15]</sup> appears to be relatively spared compared with that in AD. Lim *et al.*<sup>[15]</sup> found that reduced glucose metabolism in the medial occipital area and the cingulate island is a highly specific sign of DLB, with specificities of 97% and 100%, respectively, while the sensitivity of visual inspection ranged from 43% to 50% for the medial occipital and from 62% to 86% for the cingulate island.

Using VBM with VSRAD®, Nakatsuka *et al.*<sup>[16]</sup> examined its ability to discriminate between DLB and AD. Atrophy in the midbrain, pons, and cerebellum was

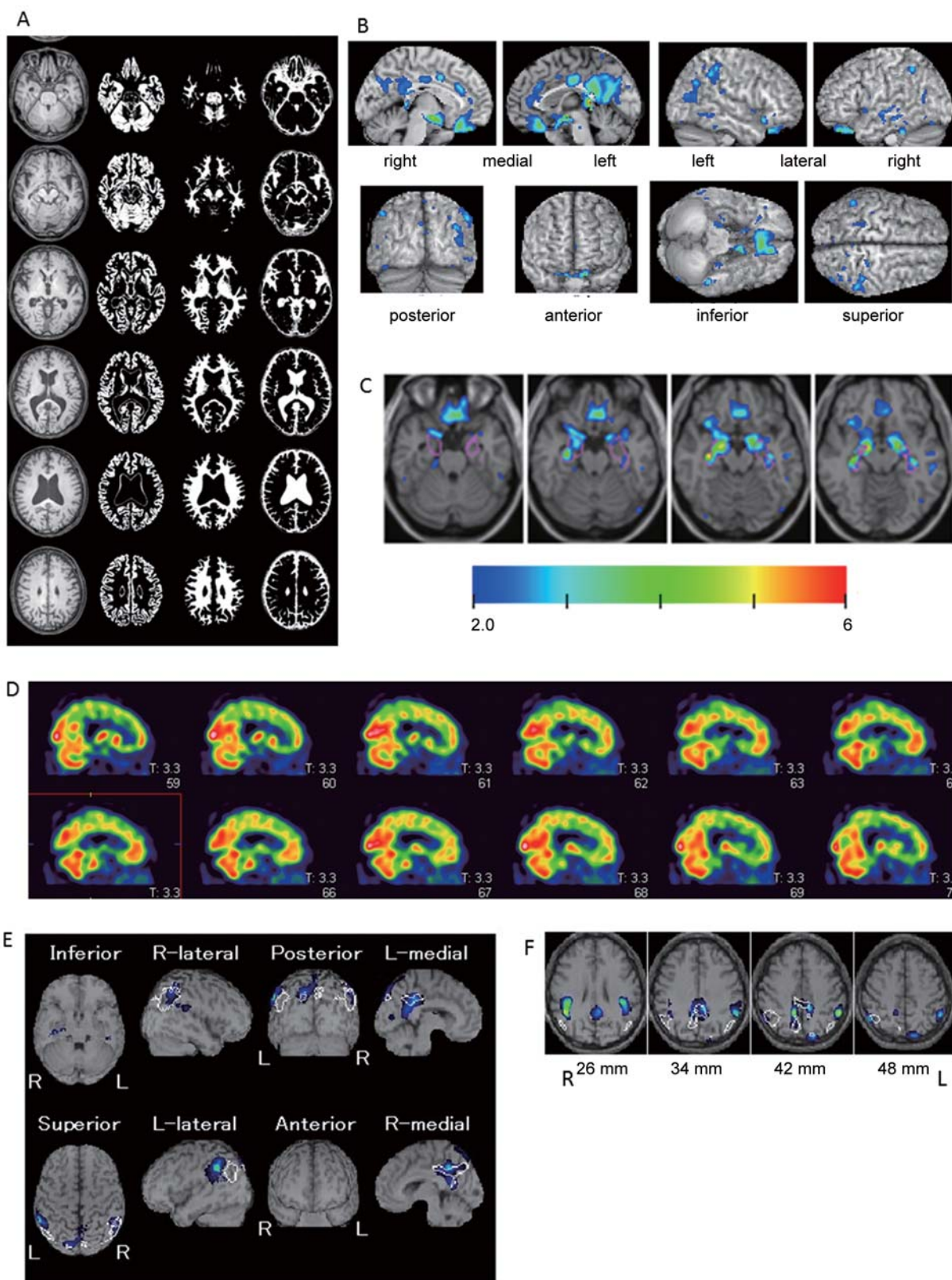


**Fig. 2.** A clinical case of suspected Alzheimer's disease (AD). A–C: VBM analyzed with VSRAD®. A: Segmented results for quality check of the procedure. Left column: original transaxial MR images; next 3 columns: extracted gray matter, white matter, and cerebrospinal fluid images, respectively. B: Z-scores superimposed on the cortical surface T1-weighted 3D volume MR image. C: Z-scores superimposed on the transaxial T1-weighted MR image. Purple VOIs indicate voxels with significant volume reduction in early AD by group comparison. D–F: Z-score analysis with eZIS. D: <sup>99m</sup>Tc-ethylcysteinate dimer SPECT sagittal images from the same patient. E: Z-scores calculated from SPECT superimposed on the cortical surface T1-weighted 3D volume MR image. F: Z-scores calculated from SPECT superimposed on the transaxial T1-weighted MR image. White VOIs indicate voxels with significant volume reduction in early AD by group comparison.

observed as white matter atrophy in DLB compared with AD. Using averaged Z-scores in VOIs in the midbrain, ROC analysis showed a sensitivity of 80%, a specificity of 64%, and an accuracy of 72%<sup>[16]</sup> for discrimination of DLB from AD.

### **Differential Diagnosis of Frontotemporal Lobe Degeneration: Progressive Supranuclear Palsy versus Corticobasal Syndrome**

Corticobasal disease (CBD) and progressive supranuclear palsy (PSP) are difficult to diagnose because of the wide variety of symptoms and overlaps in symptoms and neurological findings. Sakurai *et al.*<sup>[17]</sup> evaluated the utility of white-matter atrophy to differentiate patients with clinically diagnosed CBD (corticobasal syndrome, CBS) and PSP (Richardson's syndrome, RS). They found that with the target VOIs for CBS in the bilateral frontal white matter, the two diseases are discriminated with sensitivity of 89%, specificity of 100%, and accuracy of 96% with a cutoff Z-score of 1.30, and with the target VOI for RS in the midbrain, they were discriminated with sensitivity of 81%, specificity of 81%, and accuracy of 81% with a cutoff Z-score of 0.97.

### **New Findings Owing to Technology Development**

Recently, the resolution of medical equipment and the precise procedures for image analysis have progressed tremendously. With these methods, particularly DARTEL for normalization, we compared the longitudinal reduction of glucose metabolism in AD patients and cognitively normal volunteers. With DARTEL, precise anatomical normalization generates relatively homogeneously-shaped images. Nine <sup>11</sup>C-PiB-positive AD patients and 10 <sup>11</sup>C-PiB-negative normal volunteers were studied. Two <sup>18</sup>F-FDG PET scans were performed at an interval of 12 months, and all images were spatially normalized using the DARTEL

algorithm and analyzed with SPM8. The one-year reduction of glucose metabolism in AD patients was significantly greater in the area surrounding the orbital sulcus, including from the subgenual area to the anterior olfactory nucleus (AON) in addition to the posterior cingulate and medial temporal lesions, where decreases in glucose metabolism have been described (Fig. 3). Fouquet *et al.*<sup>[18]</sup> reported that although the largest annual decrease in metabolism occurs in the posterior cingulate-precuneus area, patients who convert to AD have a significantly greater decrease than non-converters in two ventro-medial prefrontal areas, the subgenual (BA25) and anterior cingulate (BA24/32). Moreover, Villain *et al.*<sup>[19]</sup> suggested that hippocampal atrophy in AD patients progressively leads to disruption of the cingulum bundle and uncinate fasciculus, which in turn leads to glucose hypometabolism in the cingulate and subgenual cortices. We speculate that the AON may be included in this subgenual area where decreased metabolism occurs<sup>[20]</sup>. Pathologically, amyloid deposition and neurofibrillary changes have been reported in the AON of AD patients. The AON has connections to the piriform cortex, anterior amygdala, periamygdaloid cortex, rostral entorhinal cortex, hypothalamus, and habenula. Due to these pathways, the AON is rich in dendrites and astrocytes, resulting in abundant glucose consumption in this small region. We also speculate that reduction of glucose metabolism in the AON is responsible for the olfactory disturbances in AD patients.

### **Prospective Application of Neurostatistical Imaging**

Brain CT has more homogeneity and less distortion than MRI, even when using different machines or scan protocols. It is also relatively economical and widely available. Moreover, nowadays, CT data are easily available from

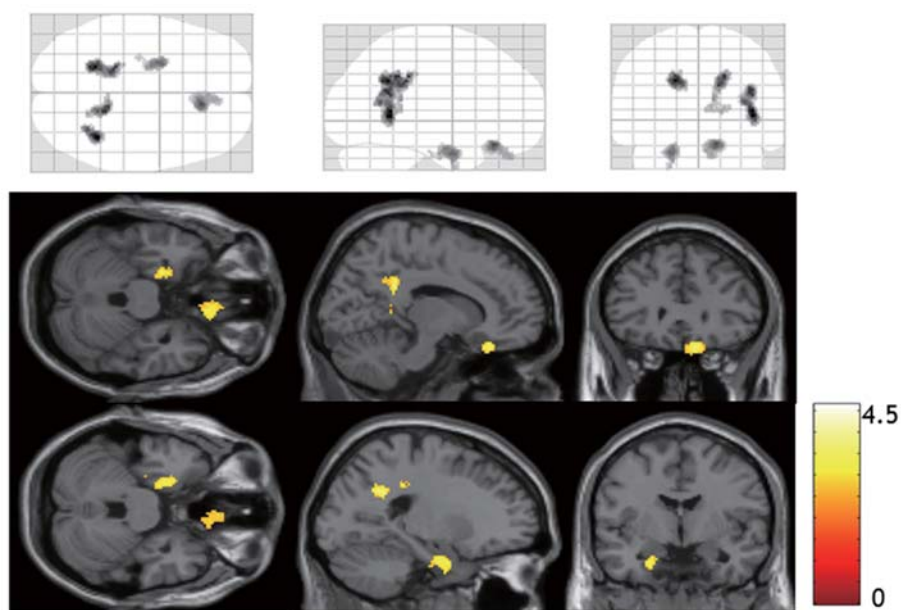


Fig. 3. One-year reduction of glucose metabolism is proportionally greater in Alzheimer’s disease (AD) patients than in cognitively normal volunteers. The one-year proportional reduction of glucose metabolism was significantly greater in AD patients than in controls in the bilateral posterior cingulate gyri, right precuneus, bilateral parahippocampal gyri, left amygdala, right rectal gyrus, and medial orbital gyrus, including caudal to the right rectal gyrus and the olfactory sulcus corresponding to the right olfactory tract (threshold at uncorrected  $P < 0.01$ ;  $k > 150$  voxels). The SPM of the  $t$ -statistics is displayed in a standard format as a maximum intensity projection viewed from the top, right-hand side and the back (top three images from left to right respectively), and as orthogonal sections (middle and bottom ranks).

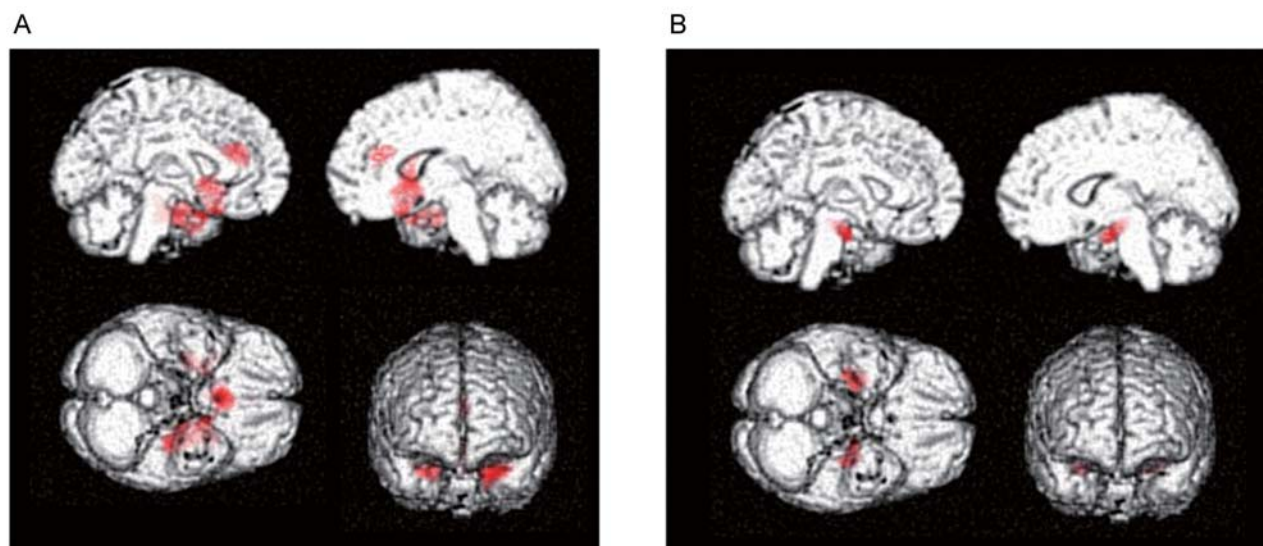
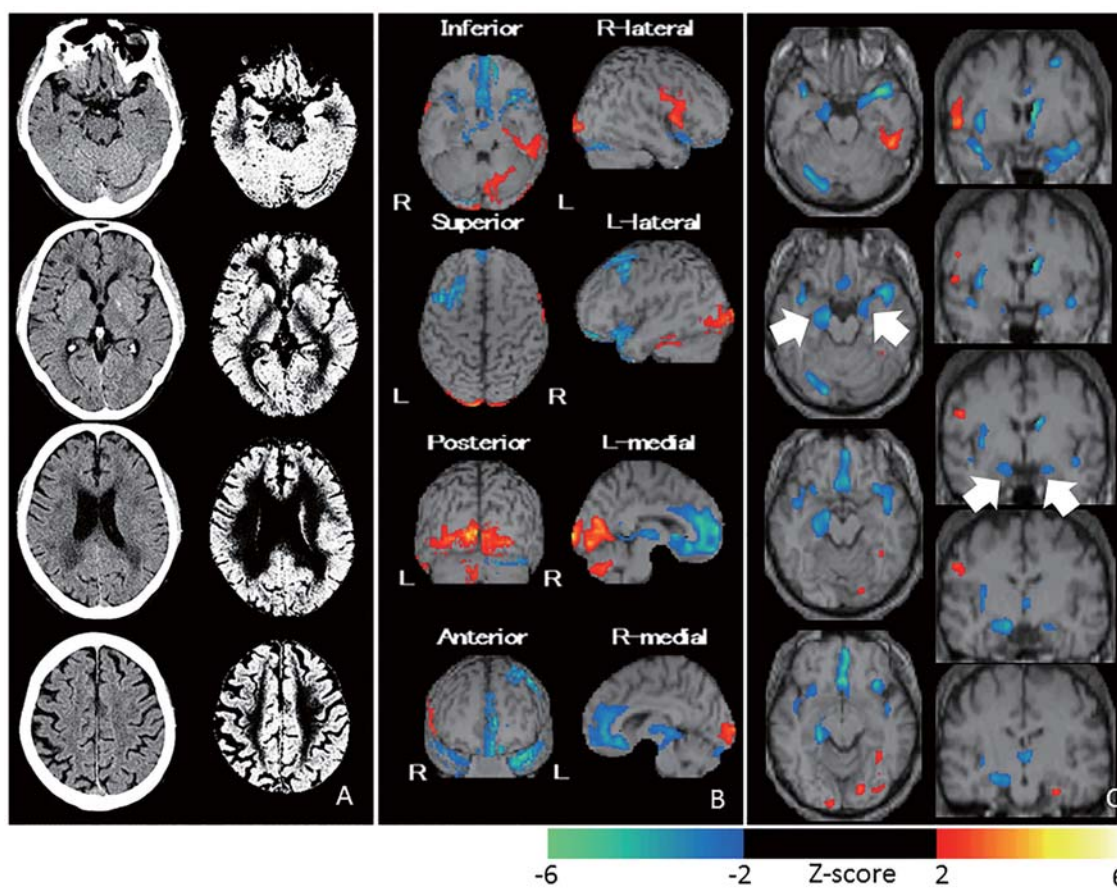


Fig. 4. A: Significant reduction of regional gray matter volume in the bilateral medial temporal cortex, temporopolar areas, right caudate, and anterior cingulate in Alzheimer’s disease (AD) patients with CT-VBM. Significance maps of decreased gray matter volume in AD patients superimposed on a T1-weighted surface MRI template image in MNI space. B: Significant reduction of regional gray matter volume in the bilateral medial temporal cortex in AD patients with MR-VBM. Significance maps of decreased gray matter volume in AD patients superimposed on a surface T1-weighted MRI template image in MNI space.

routine PET/CT studies. We compared the results from CT-VBM with those from MRI-based VBM (MR-VBM) in the same individuals<sup>[21]</sup>. All of the AD patients showed positive <sup>11</sup>C-PiB accumulation and none of the cognitively normal controls showed an accumulation. In CT-VBM, the AD group showed a significant decrease of gray matter volume in the bilateral entorhinal cortex, left hippocampus, left anterior cingulate gyrus, right temporopolar area, and right head of the caudate, compared to a cognitively normal group (Fig. 4). In MR-VBM, the AD group showed a significant decrease of gray matter volume in the bilateral hippocampus and left entorhinal cortex at BA28 compared to the cognitively normal group (Fig. 4). The most significant atrophy was observed in the left hippocampus.

The results of Z-score analysis comparing one <sup>11</sup>C-PiB positive AD patient with a normal database are shown in Figure 5. The normal database was constructed with gray matter extracted from CT images. Blue color in bilateral medial temporal regions shows significant volume reduction in this AD patient's CT image.

Although for clinical use, a simpler and proper program for CT-VBM or an advanced scanning technique for more precise tissue contrast without heavier radiation exposure is desirable, our results suggest that CT-VBM has the potential to replace MR-VBM for diagnosing AD. Moreover, the cortical gray matter volume from CT can also be used for partial volume correction (PVC); especially in amyloid imaging, PVC may be necessary for accurate assessment



**Fig. 5.** CT-based VBM. **A:** CT images from an <sup>11</sup>C-PiB-positive 60-year-old female AD patient. Left column, original CT images; right column, segmented gray matter from CT images. **B and C:** Z-scores obtained from gray matter image in **A** superimposed on the cortical surface (**B**) and transaxial and coronal (**C**) images of a T1-weighted 3D volume MR image in MNI space. Warm color indicates increase and cool color indicates decrease. That is, blue color in bilateral medial temporal regions (white arrow) shows significant volume reduction in this AD patient's CT image.

of the increased accumulation in the atrophied brain in AD. Without PVC, more atrophied brain in AD patients than in healthy volunteer shows underestimation of PiB accumulation. The availability of PET/CT scanners allows the application of PET data with CT-based PVC and VBM for patients with a single visit. Furthermore, when PET/MRI is used more frequently, these PVC and VBM procedures can be more precisely and easily approached.

## Conclusion

In diagnosing neurodegenerative dementia, recently many procedures using new technology like machine learning have been developed. In the near future, better procedures for automatic diagnosis may be developed. At present, as shown in this article, Z-score analysis of each patient's image is useful for routine clinical use, especially after the diagnostic accuracy is estimated. This can be used for both anatomical and metabolic images.

Many artifacts can occur in these traditional procedures due to mis-segmentation, mis-registration, normalization errors, and calculation errors. Accordingly, when neurostatistical imaging is used, it should always be compared to the original tomographic images to confirm a tendency in the neurostatistical analysis. Inconsistencies should be further investigated. When neurostatistical imaging is used adequately, much useful and beneficial information is revealed.

Received date: 2014-04-30; Accepted date: 2014-06-14

## REFERENCES

- [1] Minoshima S, Frey KA, Koeppe RA, Foster NL, Kuhl DE. A diagnostic approach in Alzheimer's disease using three-dimensional stereotactic surface projections of fluorine-18-FDG PET. *J Nucl Med* 1995, 36: 1238–1248.
- [2] Kobayashi S, Tateno M, Utsumi K, Takahashi A, Morii H, Saito T. Two-layer appearance on brain perfusion SPECT in idiopathic normal pressure hydrocephalus: a qualitative analysis by using easy Z-score imaging system, eZIS. *Dement Geriatr Cogn Disord* 2009, 28: 330–337.
- [3] Minoshima S, Foster NL, Kuhl DE. Posterior cingulate cortex in Alzheimer's disease. *Lancet* 1994, 344: 895.
- [4] Ohnishi T, Matsuda H, Tabira T, Asada T, Uno M. Changes in brain morphology in Alzheimer disease and normal aging: is Alzheimer disease an exaggerated aging process? *AJNR Am J Neuroradiol* 2001, 22: 1680–1685.
- [5] Klunk WE, Engler H, Nordberg A, Wang YM, Blomqvist G, Holt DP, *et al.* Imaging brain amyloid in Alzheimer's disease with Pittsburgh Compound-B. *Ann Neurol* 2004, 55: 306–319.
- [6] Maruyama M, Shimada H, Suhara T, Shinotoh H, Ji B, Maeda J, *et al.* Imaging of tau pathology in a tauopathy mouse model and in Alzheimer patients compared to normal controls. *Neuron* 2013, 79: 1094–1108.
- [7] Ashburner J, Friston KJ. Voxel-based morphometry - The methods. *Neuroimage* 2000, 11: 805–821.
- [8] Minoshima S, Giordani B, Berent S, Frey KA, Foster NL, Kuhl DE. Metabolic reduction in the posterior cingulate cortex in very early Alzheimer's disease. *Ann Neurol* 1997, 42: 85–94.
- [9] Kogure D, Matsuda H, Ohnishi T, Asada T, Uno M, Kunihiro T, *et al.* Longitudinal evaluation of early Alzheimer's disease using brain perfusion SPECT. *J Nucl Med* 2000, 41: 1155–1162.
- [10] Hirata Y, Matsuda H, Nemoto K, Ohnishi T, Hirao K, Yamashita F, *et al.* Voxel-based morphometry to discriminate early Alzheimer's disease from controls. *Neurosci Lett* 2005, 382: 269–274.
- [11] Imabayashi E, Matsuda H, Asada T, Ohnishi T, Sakamoto S, Nakano S, *et al.* Superiority of 3-dimensional stereotactic surface projection analysis over visual inspection in discrimination of patients with very early Alzheimer's disease from controls using brain perfusion SPECT. *J Nucl Med* 2004, 45: 1450–1457.
- [12] Kawachi T, Ishii K, Sakamoto S, Sasaki M, Mori T, Yamashita F, *et al.* Comparison of the diagnostic performance of FDG-PET and VBM-MRI in very mild Alzheimer's disease. *Eur J Nucl Med Mol Imaging* 2006, 33: 801–809.
- [13] Matsuda H, Mizumura S, Nagao T, Ota T, Iizuka T, Nemoto K, *et al.* Automated discrimination between very early Alzheimer disease and controls using an easy Z-score imaging system for multicenter brain perfusion single-photon emission tomography. *Am J Neuroradiol* 2007, 28: 731–736.
- [14] Mito Y, Yoshida K, Yabe I, Makino K, Hirotani M, Tashiro K, *et al.* Brain 3D-SSP SPECT analysis in dementia with Lewy bodies, Parkinson's disease with and without dementia, and Alzheimer's disease. *Clin Neurol Neurosurg* 2005, 107: 396–403.
- [15] Lim SM, Katsifis A, Villemagne VL, Best R, Jones G, Saling M, *et al.* The <sup>18</sup>F-FDG PET cingulate island sign and comparison to <sup>123</sup>I-β-CIT SPECT for diagnosis of dementia with Lewy bodies. *J Nucl Med* 2009, 50: 1638–1645.
- [16] Nakatsuka T, Imabayashi E, Matsuda H, Sakakibara R, Inaoka T, Terada H. Discrimination of dementia with Lewy bodies from Alzheimer's disease using voxel-based morphometry of white matter by statistical parametric mapping 8 plus diffeomorphic anatomic registration through

- exponentiated Lie algebra. *Neuroradiology* 2013, 55: 559–566.
- [17] Sakurai K, Imabayashi E, Tokumaru AM, Hasebe S, Murayama S, Morimoto S, *et al.* The feasibility of white matter volume reduction analysis using SPM8 plus DARTEL for the diagnosis of patients with clinically diagnosed corticobasal syndrome and Richardson's syndrome. *Neuroimage Clin* 2014. DOI: 10.1016/j.nicl.2014.02.009
- [18] Villain N, Fouquet M, Baron JC, Mezenge F, Landeau B, de La Sayette V, *et al.* Sequential relationships between grey matter and white matter atrophy and brain metabolic abnormalities in early Alzheimer's disease. *Brain* 2010, 133: 3301–3314.
- [19] Fouquet M, Desgranges B, Landeau B, Duchesnay E, Mezenge F, de la Sayette V, *et al.* Longitudinal brain metabolic changes from amnesic mild cognitive impairment to Alzheimer's disease. *Brain* 2009, 132: 2058–2067.
- [20] Imabayashi E, Matsuda H, Yoshimaru K, Kuji I, Seto A, Shimano Y, *et al.* Pilot data on telmisartan short-term effects on glucose metabolism in the olfactory tract in Alzheimer's disease. *Brain Behav* 2011, 1: 63–69.
- [21] Imabayashi E, Matsuda H, Tabira T, Arima K, Araki N, Ishii K, *et al.* Comparison between brain CT and MRI for voxel-based morphometry of Alzheimer's disease. *Brain Behav* 2013, 3: 487–493.